Part I

A grammar of turbulence

1

Introduction

1.1 Turbulence, its community, and our approach

Even if you have not studied turbulence, you already know a lot about it. You have seen the chaotic, ever-changing, three-dimensional nature of chimney plumes and flowing streams. You know that turbulence is a good mixer. You might have come across an article that described the intrigue it holds for mathematicians and physicists.

Unless a fluid flow has a low Reynolds number or very stable stratification (less dense fluid over more dense fluid), it is turbulent. Most flows in engineering, in the lower atmosphere, and in the upper ocean are turbulent. Because of its "mathematical intractability" – turbulence does not yield exact mathematical solutions – its study has always involved observations. But over the past three decades numerical approaches have proliferated; today they are a dominant means of studying turbulent flows.

Turbulence has long been studied in both engineering and geophysics. G. I. Taylor's contributions spanned both (Batchelor, 1996). The Lumley and Panofsky (1964) work was my introduction to that breadth, but as Lumley later commented, their parts of that text "just … touch." Today the turbulence field seems more coherent than it was in 1964, although it still has subcommunities and dialects (Lumley and Yaglom, 2001).

In Part I of this book we focus on the physical understanding of turbulence, surveying its key properties. We'll use its governing equations to guide our discussions and inferences. We shall also discuss the main types of numerical approaches to turbulence. You might be concerned by our use of little mathematical "tricks" – not because they're complicated or difficult, but because you've never seen them before and might not have thought of them yourself. Don't worry: we pass them on because they are some of the useful tools developed over the many years that scholars have pondered turbulence. You can pass them on too.

Figure 1.1 Instability of an axisymmetric jet. A laminar stream of air flows from a circular tube at the left at Reynolds number 10 000 and is made visible by a smoke wire. The edge of the jet develops axisymmetric oscillations, rolls up into vortex rings, and then abruptly becomes turbulent. Photograph courtesy Robert Drubka and Hassan Nagib. From Van Dyke (1982).

1.2 The origins and nature of turbulence

Turbulent rather than smooth, *laminar* flow of a fluid, liquid or gas, normally occurs if a dimensionless flow parameter called the *Reynolds number* $Re = UL/\nu$ exceeds a critical value. Here U and L are velocity and length scales of the flow† and ν is the kinematic viscosity (dynamic viscosity μ/density ρ) of the fluid. The atmospheric boundary layer is turbulent, but as we shall see in Part II stable density stratification can strongly modulate its depth and the intensity and scale of its turbulence. Winter sunrises here in central Pennsylvania often reveal laminar chimney plumes in the very stably stratified flow caused by the overnight cooling of the earth's surface. The turbulent eddies‡ so prominent in cumulus clouds and flowing streams can be revealed in laboratory turbulence through flow-visualization techniques (Figure 1.1).

There are two types of turbulence with quite different physics. The most common type, *three-dimensional turbulence*, arises from the tendency of fluid motion of large Re to be turbulent and the tendency of turbulence to be three dimensional. But *two-dimensional turbulence* is also of interest; it causes the darting of the colors in soap films and is a model of the largest-scale motions of the atmosphere. We shall discuss it in Chapter 7.

† For example, in Figure 1.1 U is the velocity averaged over the tube cross section and L is the tube diameter.

‡ To paraphrase Batchelor (1950), "eddy" does not refer to any specific local distribution of velocity; it is simply a concise term for local turbulent motion with a certain length scale – an arbitrary local flow pattern characterized by size alone. A turbulent flow has a spectrum of eddies of different size, determined by an analysis of the velocity field into sinusoidal components of different wavelengths (Chapter 15).

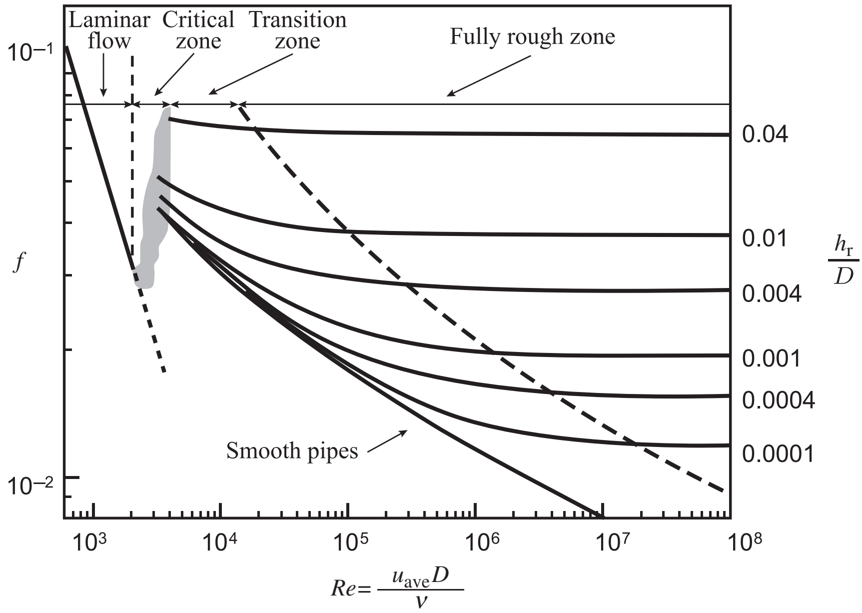

Figure 1.2 The *Moody chart*, which shows the behavior of the Darcy friction factor f, Eq. (1.5), in a circular pipe. In laminar flow $f \propto Re^{-1}$, Eq. (1.6); f jumps to larger values with the transition to turbulence at $Re \simeq 2000$, and in the region of equilibrium turbulence past the critical zone f depends also on the wall-roughness height h_r relative to D. Adapted from Moody (1944).

1.3 Turbulence and surface fluxes

An early motivation for the study of turbulence was to understand how it makes the fluxes of momentum, heat, and mass at a solid surface much larger than in the laminar case. This has important applications to both geophysical and engineering flows.

Fluid flowing through a long circular pipe becomes turbulent at some point downstream if the Reynolds number $Re = u_{\text{ave}} D/\nu$ (u_{ave} is the velocity averaged over the pipe cross section and D is the pipe diameter) exceeds about 2000. This *transition to turbulence*, as it is called, is marked by a jump in the shear stress (which is also interpretable as a momentum flux, Section 1.5) at the wall (Figure 1.2). There is a corresponding jump in the required pumping power (Problem 1.1).

To understand these abrupt changes at transition we need some background on pipe flow. In the steady, laminar case its velocity profile is parabolic (Problem 1.1),

$$u(r) = u_{\max}\left(1 - \frac{r^2}{R^2}\right), \tag{1.1}$$

where r is the radial coordinate, $R = D/2$ is the pipe radius, and $u_{\max}$ is the maximum (centerline) velocity. The velocity averaged over the cross section is

$$u_{\text{ave}} = \frac{1}{\pi R^2} \int_0^R u(r) 2\pi r \, dr = \frac{u_{\max}}{2}. \tag{1.2}$$

The wall shear stress is

$$\tau_{\text{wall}} = -\mu \left. \frac{\partial u}{\partial r} \right|_{r=R} = 8\mu \frac{u_{\text{ave}}}{D}, \tag{1.3}$$

with μ the dynamic viscosity of the fluid. Since $\partial p/\partial x$ does not depend on x (Problem 1.1), we can write the axial force balance on a slug of fluid of length L and diameter D as

$$\tau_{\text{wall}} \, \pi D L = -\frac{\partial P}{\partial x} L \frac{\pi D^2}{4}, \quad \text{so that} \quad -\frac{\partial P}{\partial x} D = 4\tau_{\text{wall}}. \tag{1.4}$$

The mean pressure gradient nondimensionalized with $\rho(u_{\text{ave}})^2/2$ and D is called the *Darcy friction factor*,†

$$f \equiv \frac{-\frac{\partial P}{\partial x} D}{\rho(u_{\text{ave}})^2/2} = \frac{4\tau_{\text{wall}}}{\rho(u_{\text{ave}})^2/2}. \tag{1.5}$$

Thus f is, from Eq. (1.3),

$$f_{\text{lam}} = \frac{64\mu u_{\text{ave}}}{D\rho(u_{\text{ave}})^2} = \frac{64}{Re}. \tag{1.6}$$

Figure 1.2 shows this inverse-Re dependence of f in the laminar-flow regime.

Past the critical zone, Figure 1.2, u_{ave} and τ_{wall} are turbulent quantities, so (as we'll discuss in detail in Chapter 2) we work with their mean values $\overline{u}_{\text{ave}}$ and $\overline{\tau}_{\text{wall}}$. In the turbulent regime Eq. (1.5) implies $\overline{\tau}_{\text{wall}} = f_{\text{turb}} \, \rho(\overline{u}_{\text{ave}})^2/8$. Therefore the ratio of the mean wall stress in turbulent pipe flow and the wall stress in laminar flow at the same average velocity is

$$\frac{\overline{\tau}_{\text{wall}}}{\tau_{\text{wall}}(\text{laminar flow})} = \frac{f_{\text{turb}}}{f_{\text{lam}}} = \frac{f_{\text{turb}} \, Re}{64}. \tag{1.7}$$

† The *Fanning friction factor* is the wall stress nondimensionalized with $\rho(u_{\text{ave}})^2/2$. The Darcy friction factor, Eq. (1.5), is larger by a factor of four.

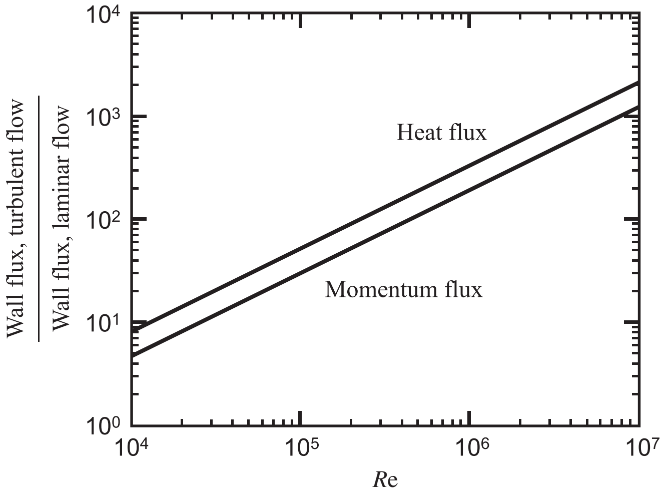

Figure 1.3 The ratios of mean fluxes at the wall in turbulent and laminar flow through smooth pipes. The momentum-flux ratio is Eq. (1.7) evaluated with f data from Figure 1.2; the heat-flux ratio is Eq. (1.16) evaluated with Nu data from Dittus and Boelter (1930), as summarized by Turns (2006).

This ratio is plotted for smooth pipes in Figure 1.3. It has very large values at large Re, indicating the strong influence of turbulence on the wall stress.

Turns (2006) shows that a good fit to the classical mean-velocity measurements of Nikuradse (1933) in turbulent pipe flow is

$$\frac{\overline{u}(r)}{\overline{u}_{\text{ave}}} = \frac{f^{1/2}}{\sqrt{2}}\left(2.5\ln\left[\frac{Re\, f^{1/2}}{2\sqrt{2}}\left(1 - \frac{r}{R}\right)\right] + 5.5\right). \tag{1.8}$$

Figure 1.4 shows that this profile is much "flatter" in the core region than the laminar profile (1.1). At large Re the mean-velocity gradient is significant only adjacent to the wall, where it is much larger than in laminar flow of the same bulk fluid velocity. The wall stress in turbulent flow is still defined by the velocity gradient at the wall, Eq. (1.3), but that gradient, and therefore the wall shear stress, fluctuates chaotically with time and with position. The mean value (which we designate by an overbar) of the wall stress is

$$\overline{\tau}_{\text{wall}} = -\mu\overline{\frac{\partial u}{\partial r}\bigg|_{r=R}} = -\mu\frac{\partial \overline{u}}{\partial r}\bigg|_{r=R}. \tag{1.9}$$

We have used the property that the differentiation and averaging can be done in either order (Problem 1.3). The sharp increase in the mean-velocity gradient at the wall at transition (Figure 1.4) causes a sharp increase in wall stress (Figure 1.2).

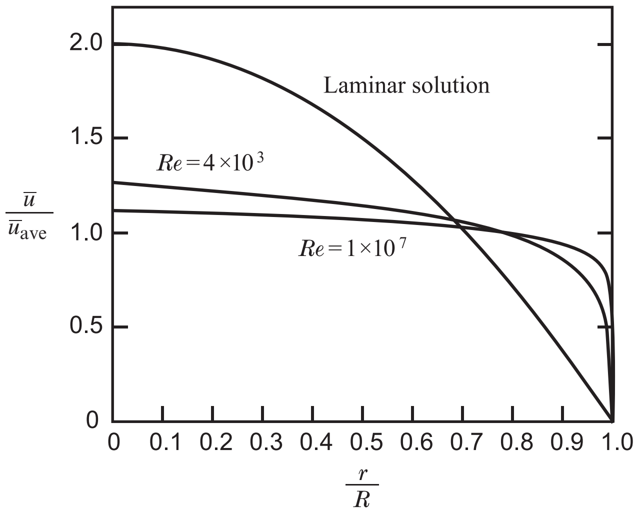

Figure 1.4 Profiles of $\overline{u}/\overline{u}_{ave}$ in turbulent pipe flow, Eq. (1.8), "flatten" as the Reynolds number increases, making the mean shear and mean stress at the wall much larger than in laminar flow with the same average velocity.

Pipes typically have some wall roughness, and Figure 1.2 indicates that the mean wall stress increases with that roughness. The explanation (Kundu, 1990) is that immediately adjacent to the wall in turbulent pipe flow is a *laminar sublayer* of thickness $\delta \sim 5\nu/u_*$, with $u_* = (\overline{\tau}_{wall}/\rho)^{1/2}$ the *friction velocity*. If the typical height h_r of the individual "bumps" or *roughness elements* on the wall is much less than δ, wall roughness has minimal effect and the mean wall stress is the viscous one given by Eq. (1.9). But as h_r approaches δ the roughness elements cause *form drag* through the pressure distribution on their surface, which adds to the viscous drag and increases the friction factor f. When h_r is large enough this form drag dominates and f ceases to change with Re, as indicated in Figure 1.2.

An analogous situation exists for the wall heat flux H_{wall} (watts m^{-2}). It is carried entirely by the molecular diffusion process called *conduction heat transfer*:

$$H_{wall} = -k\frac{\partial T}{\partial r}\bigg|_{r=R}, \tag{1.10}$$

with k the thermal conductivity (watts m^{-1} K^{-1}). The heat flux is continuous at the fluid–wall interface, but the temperature gradient there is discontinuous if k of the wall material and the fluid differ. We shall consider the fluid side.

The temperature profile in fully developed laminar pipe flow depends on the temperature boundary conditions. We'll consider the analytically simple case where the fluid and wall temperatures vary linearly with x but their difference, and the wall heat flux, are independent of x. Its temperature profile is (Problem 1.2)

$$T(0,x) - T(r,x) = -\frac{R^2 u_{\text{ave}}}{\alpha}\frac{\partial T}{\partial x}\left[\frac{r^2}{2R^2}\left(1 - \frac{r^2}{4R^2}\right)\right], \tag{1.11}$$

with $\alpha = k/(\rho c_p)$ the thermal diffusivity of the fluid. The relation between the wall heat flux and $\partial T/\partial x$ is (Problem 1.2)

$$H_{\text{wall}} = -\frac{D u_{\text{ave}} \rho c_p}{4}\frac{\partial T}{\partial x}, \tag{1.12}$$

so the temperature profile (1.11) can be rewritten as

$$T(0,x) - T(r,x) = \frac{H_{\text{wall}} D}{k}\left[\frac{r^2}{2R^2}\left(1 - \frac{r^2}{4R^2}\right)\right]. \tag{1.13}$$

The wall heat flux made dimensionless with pipe diameter D, fluid thermal conductivity k, and a temperature difference ΔT is called a Nusselt number Nu:

$$Nu = \frac{H_{\text{wall}} D}{k \Delta T}. \tag{1.14}$$

ΔT is defined through the wall temperature $T_{\text{w}}(x)$ and the "bulk fluid temperature" at that position, $T_{\text{b}}(x)$:

$$T_{\text{b}}(x) = \frac{\int_0^R u(r)\, T(r,x)\, 2\pi r\, dr}{\pi R^2 u_{\text{ave}}}, \quad Nu = \frac{H_{\text{wall}} D}{k(T_{\text{b}} - T_{\text{w}})}. \tag{1.15}$$

Turns (2006) shows that in the laminar case in this problem $Nu \simeq 4.4$.

In the turbulent case the heat flux at a point on the wall, like the stress there, fluctuates chaotically in time. The turbulent mixing makes the mean temperature gradient relatively small over most of the cross section; it is large only near the wall, as for velocity (Figure 1.4). The mean wall heat flux, the product of the fluid thermal conductivity k and the mean temperature gradient at the wall, is much larger than in the laminar case.

From Eq. (1.14) in this problem we can write the ratio of wall heat fluxes as, for given values of D, k, and ΔT,

$$\frac{\overline{H}_{\text{wall}}}{H_{\text{wall}}(\text{laminar flow})} = \frac{Nu}{Nu(\text{laminar flow})} = \frac{Nu}{4.4}. \tag{1.16}$$

Figure 1.3 shows the wall-flux ratios in the turbulent regime. The ratios for heat and momentum differ by a constant factor of about 1.5–2 (a manifestation of the *Reynolds analogy* between heat and momentum transfer) as they increase sharply with Reynolds number.

If the flow over the earth's surface were laminar, not turbulent, the environmental effects would be profound. In clear summer weather, for example, the earth's surface temperature could routinely approach 100 °C during the day and 0 °C at night (Chapter 9).

1.4 How do we study turbulence?

Turbulence has long had a special attraction for physicists and mathematicians; it has been called "the last great unsolved problem of classical physics."[†] In practical terms this means that we cannot analytically solve the equations of turbulent fluid motion. The difficulty stems from their nonlinearity.

Leonardo da Vinci sketched turbulent water flows, and reportedly gave the sage advice: "Remember when discoursing on the flow of water to adduce first experience and then reason."[‡] Even today, some 500 years after da Vinci, much of our understanding of turbulence is rooted in observations.

Since the 1960s turbulence has been studied numerically as well. One early study had a revolutionary impact. Lorenz (1963) discovered the profound effects of very small changes in initial conditions on the behavior of a very simplified, three-equation, nonlinear model of turbulent convection. He found that two solutions with slightly different initial conditions diverged with time. This *sensitive dependence on initial conditions* is now recognized as a fundamental property of turbulence. Gleick (1987) describes Lorenz' findings as the beginning of the field now called *chaos*.

The advances in digital computers and numerical techniques for solving differential equations after Lorenz' early work soon allowed the *numerical simulation* of turbulence. There are two varieties. *Direct numerical simulation* (DNS) is the numerical solution of the governing fluid equations. It is (within the numerical approximations used) exact, but it is possible only in low Reynolds number flows (Problem 1.9). The Orszag–Patterson (1972) $32 \times 32 \times 32$ (32^3) calculation of isotropic turbulence is considered the first DNS. *Large-eddy simulation* (LES) is an approximate technique that solves for the largest-scale structure of turbulence fields; its underlying concepts were laid out by Lilly (1967). Deardorff's (1970a) study of turbulent channel flow on a $24 \times 14 \times 20$ grid mesh (6720 grid points) is widely

[†] According to Holmes *et al*. (1996), precise references to such remarks are elusive. They have been attributed to Sommerfeld, Einstein, and Feynman, and beginning in 1895 Horace Lamb expressed similar sentiments in his *Hydrodynamics*.

[‡] Rouse and Ince (1957) state that this quote appears in the Carusi and Favaro (1924) republication of da Vinci's writings.